Electromagnetic-Transient analysis in the Laplace-domain through the QD algorithm

L.J. Castañón, J. L. Naredo, J. R. Zuluaga, Martin G. Vega.

Abstract.- **The Frequency-Domain (FD) Electromagnetic Transient (EMT) analysis of power systems (PS) is often performed using the Windowed Numerical Laplace Transform (W-NLT) method. For practical analysis, this method provides adequate accuracy at moderate computational costs. Nevertheless, research applications often require much higher accuracy levels, and the W-NLT method has proven computationally expensive and unreliable. This paper, therefore, presents the Quotient-Difference (QD) NLT method as a complement and as an alternative to the W-NLT method, particularly for research tasks in PS-EMT analysis. The QD-NLT method is analyzed thoroughly here and is applied to test cases to demonstrate its effectiveness.**

Keywords.- **Frequency domain (FD) analysis, Numerical Laplace Transform (NLT), Quotient-Difference (QD) algorithm, rational functions, continued fractions, Electromagnetic Transients (EMTs).**

I. INTRODUCTION.

Frequency-domain (FD) methods are often used for analyzing power-system (PS) electromagnetic-transients (EMTs) to complement and validate their time-domain (TD) counterparts, such as EMTP methods. The most widely used FD method for this application is perhaps the Numerical Laplace Transform (NLT) technique [1,2,3,5,11]. As this is based on truncation of the Laplace inversion-integral by means of a data window, referred to here as the Windowed Numerical Laplace Transform (W-NLT).

The accuracy attained with the W-NLT typically is in the range of relative errors— between 1.0e-3 and 1.0e-5, which is appropriate for most engineering applications in EMT analysis; nevertheless, there are situations that require much greater accuracies. This is the case in research and development (R&D) activities in EMT analysis. The authors of this paper have been able to attain accuracy levels up to 1.0e-9 with the W-NLT, but only in certain cases and only by increasing 1024 times the number of regular computations [6]. The authors of this paper have thus been engaged in the search for other NLT methods capable of delivering higher levels of accuracy at moderate computational costs. The purpose of this paper is to introduce a Numerical Laplace Transform inversion method based on the Quotient-Difference (QD) algorithm [7], primarily as an R&D tool in EMT analysis. This method is referred to here as QD-NLT.

L. J. Castañón, J. L. Naredo, J. R. Zuluaga,, Martin G. Vega; Cinvestav, Unidad Guadalajara, Zapopan, 45019, México.

ldcastatnon@gdl.cinvestav.mx, jzuluaga@gdl.cinvestav.mx, jlnaredo@gdl.cinvestav.mx, mvega@gdl.cinvestav.mx.

In 1954, Heinz Rutishauser proposed the QD algorithm as a major breakthrough for accelerating the convergence of infinite-series [8]. In 1982, F. R. De Hoog et al., proposed a method for numerically solving the Laplace inversion-integral through QD acceleration [7].In 2001, L. Brancik combined the Fast Fourier Transform (FFT) and the QD algorithms to numerically solve the Laplace inversion-integral, attaining both high accuracy and high computational efficiency. Brancik further applied this method to the solution of transients in constant-parameter (CP) transmission-line models [14].

This paper is organized as follows: First, the direct and inverse Laplace integrals are introduced. Then, the basics for numerical treatment of the Laplace inversion-integral are provided. Next, the standard W-NLT method is briefly explained. After that, the QD-NLT method is presented, with the aim of providing a clear and straightforward explanation. Next, the QD-NLT method is applied to a Laplace-domain function of a known time-domain solution in order to show its performance in terms of accuracy and computational efficiency; comparisons are made here with the W-NLT. Next, the QD-NLT is applied to two PS-EMT cases, one involving a multi-conductor transmission-line and the other, an underground transmission cable. Frequency-dependent parameters are considered in these two latter cases and comparisons are further made with both the W-NLT and the EMTP-rv® program. It can be concluded that the QD-NLT method is appropriate for R&D tasks in PS-EMT analysis.

II. LAPLACE INTEGRALS.

Let $f(t)$ be a causal function of the time variable *"t"*; (*i.e.*, $f(t) = 0$ for *t<0*). Its Laplace transform *F(s)* is

$$F(s) = \int_0^\infty f(t)\, e^{-st} dt, \qquad (1)$$

where *"s =c + jω"* is the Laplace complex variable whose imaginary part is identified with the angular frequency, while its real part *"c"* is usually considered constant and regarded as a damping coefficient [9].

According to Systems theory [9], both systems and their associated signals can be represented as functions of time whose relations are given in terms of convolution operations. In the Laplace-domain, time-domain convolutions are equivalent to multiplications, and transient responses can be obtained by means of algebraic methods. These responses, however, must still be transformed into time-domain through the Laplace-inversion integral:

$$f(t) = \frac{e^{ct}}{2\pi} \int_{-\infty}^{\infty} F(c + j\omega)\, e^{j\omega t} d\omega \qquad (2)$$

Time-domain functions related to physical systems are real and causal. The inversion integral (2) can thus take the following form as well:

$$f(t) = \frac{e^{ct}}{\pi} Re\left\{ \int_{0}^{\infty} F(c + j\omega)\, e^{j\omega t} d\omega \right\} \qquad (3)$$

Either expression, (2) or (3) can serve as basis for the numerical inversion of Laplace transforms.

III. NUMERICAL TREATMENT OF THE LAPLACE INVERSION-INTEGRAL.

3a) Frequency-domain discretization and time-domain aliasing.

Expression (3) is adopted here for a numerical method for inverting Laplace transforms. Let the continuous variable "ω" be replaced by the discrete one "$k\Delta\omega$", with "k" as an integer and "$\Delta\omega$" as a fixed frequency-step. Integral (3) is thus approximated as follows:

$$\tilde{f}(t) = \frac{\Delta\omega \times e^{ct}}{\pi} Re\left\{ \sum_{k=0}^{\infty} F_k e^{jk\Delta\omega t} \right\} \qquad (4a)$$

where

$$F_k = \begin{cases} F(c)/2, & k = 0 \\ F(c + jk\Delta\omega), & k = 1, 2, \dots \end{cases} \qquad (4b)$$

$\tilde{f}(t)$ in (4b) aims to be the closest possible approximation to $f(t)$. Nevertheless, it can be shown that "$\exp(-ct) \times \tilde{f}(t)$" is a periodic function with the fundamental period

$$T = 2\pi/\Delta\omega \qquad (5)$$

The periodicity of "$\exp(-ct) \times \tilde{f}(t)$" implies that $\tilde{f}(t)$ can provide an adequate approximation to $f(t)$ only within the t-interval *[0,T]*, at most. Moreover, it can be further shown that inside this interval [7]

$$\tilde{f}(t) = f(t) + \epsilon_{al} \qquad (6)$$

with

$$\epsilon_{al} = \sum_{i=1}^{\infty} e^{-icT} f(t + iT) \qquad (7)$$

Clearly, ϵ_{al} is an aliasing error in time-domain and is caused by discretization (or sampling) of $F(c + j\omega)$ in (4b). It follows from (7) that, in principle, ϵ_{al} can be made as small as desired by the proper choice of damping coefficient c.

3b) Time-domain discretization.

Now, let the continuous variable "t" be replaced by the discrete one "$t_n = n\Delta t$", with $n = 0, 1, 2, \dots N$ and Δt as a fixed discretization time-step of size

$$\Delta t = T/N \qquad (8)$$

It must be emphasized here that Δt should comply with the Nyquist sampling principle [10]. When considering (5), (6), and (8), expression (4a) is written in the following form:

$$\tilde{f}_n = f_n + \epsilon_{al} = \frac{2e^{ct}}{\Delta t} Re\left\{ \frac{1}{N} \sum_{k=0}^{N-1} F_k e^{j2\pi kn/N} \right\} + \epsilon_{trnc} \qquad (9)$$

where $\tilde{f}_n = f(n\Delta t)$, $f_n = f(n\Delta t)$ and ϵ_{trnc} is the truncation-error caused when the infinite sum in (8) is replaced by the finite one of its first N samples; *i.e.*:

$$\epsilon_{trnc} = \frac{2e^{ct}}{\Delta t} Re\left\{ \frac{1}{N} \sum_{k=N}^{\infty} F_k e^{2\pi jkn/N} \right\} \qquad (10)$$

IV. WINDOWED NLT.

As note above, aliasing error ϵ_{al} can be damped by the proper choice of a damping coefficient "c". If the time function of interest $f(t)$ is bounded, which is always the case in power-systems, a suitable value for c is given by [3]

$$c = -\frac{ln(\epsilon)}{T} \qquad (11)$$

where ϵ is a target-bound for the relative aliasing-error [3].

Truncation error ϵ_{trnc} appears in the form of Gibbs' oscillations superimposed over the retrieved function f_n in (9) [11]. Gibbs' oscillations can be attenuated substantially by the application of a data window; thus,

$$f_n \cong \frac{2}{\Delta t} Re\left\{ \frac{1}{N} \sum_{k=0}^{N-1} F_k \sigma_k e^{\frac{2\pi jkn}{N}} \right\}, \qquad (12)$$

where σ_k represents the selected data-window. The Von Hann (or Hanning) window has proven highly convenient in practical analyses [11]:

$$\sigma_k = \frac{1}{2}\left[cos\left(\frac{\pi k}{N} \right) + 1 \right]$$

Expression (12) corresponds to the Windowed Numerical Laplace Transform (W-NLT) being applied elsewhere for frequency-domain PS-EMT analysis [11]. Note that the term in brackets at (12) is an Inverse Discrete Fourier Transform (IDFT), which is evaluated with high numerical efficiency using the Inverse-Fast-Fourier-Transform algorithm (*IFFT*) [15].

V. QUOTIENT DIFFERENCE NLT

The summation in brackets at (9), without truncation, is written as follows:

$$g(z) = \sum_{k=0}^{\infty} c_k z^k \qquad (13)$$

where $c_k = F_k$ and $z = e^{2\pi jn/N}$. Function $g(z)$ can be approximated either by a partial sum of its first M terms

$$g(z) \cong \sum_{k=0}^{M} c_k z^k \qquad (14)$$

or by a rational function of the following form:

$$g(z) \cong \frac{A_M(z)}{B_M(z)} = \frac{\sum_{k=0}^{M} a_k z^k}{\sum_{k=0}^{M} b_k z^k} \qquad (15)$$

Mention is made here that (15) corresponds to the *M-th* diagonal term in a Padè table [14]. Rational approximations, such as (15), converge much faster to $g(z)$ than partial sum (14) [14]. It can thus be considered that (15) provides a technique for accelerating the convergence of infinite series (13) [15]. The key-issue is to devise a fast method to evaluate (15).

An alternate form for (14) is its continued-fraction expansion:

$$g(z) = \cfrac{d_0}{1 + \cfrac{d_1 z}{1 + \cfrac{d_2 z}{1 + \cfrac{d_3 z}{1 + \cdots \cfrac{d_{M-1}}{1 + d_M z}}}}} \qquad (16)$$

The following notation is commonly used to represent continued fractions in compact form [12]:

$$g(z) = \frac{d_0}{1} + \frac{d_1 z}{1} + \frac{d_2 z}{1} + \cdots + \frac{d_{M-1} z}{1 + d_M z} \qquad (17)$$

Coefficients d_k, with $k = 1, 2, \dots M$, can be derived from the c_ks in (14) using the QD-algorithm [13]. This is described below and illustrated in Fig. 1 for the *M=6* case.

Figure 1. Depiction of the QD method for the M=6 case.

First, assume that *M* is an even number (*i.e.*, *M=2J*); then, build a first column with elements $e_0^i = 0$, for $i = 1, 2, \dots, M - 1$, as in Fig. 1; next, build a second column with elements $q_0^i = c_{i+1}/c_i$, for $i = 0, 1, 2, \dots, M - 1$, as in Fig. 1 ; then, build the alternating following columns for elements $e_r^{(i)}$ and $q_r^{(i)}$ using the following recursive expressions:

$$e_r^{(i)} = q_r^{(i+1)} - q_r^{(i)} + e_{r-1}^{(i+1)};$$
$$r = 1, \dots, J; \quad i = 0, \dots, M - 2r \qquad (18)$$

$$q_r^{(i)} = q_{r-1}^{(i+1)} e_{r-1}^{(i+1)} / e_{r-1}^{(i)};$$
$$r = 2, \dots, J; \quad i = 0, \dots, M - 2r - 1 \qquad (19)$$

Once the *M* columns of alternating terms $e_r^{(i)}$ and $q_r^{(i)}$ have been obtained, the d_k terms for the continued-fraction expansion are retrieved from these columns through the following relations:

$$d_0 = c_0, d_{2r} = -e_r^0, r = 1, \dots, J \qquad (20)$$

$$d_{2r-1} = -q_r^0, r = 1, \dots, J \qquad (21)$$

The polynomials $A_M(z)$ and $B_M(z)$ from the rational form (15) comply with the following recursive relations involving the previously obtained d_k terms [7]:

$$A_m(z) = A_{m-1}(z) + d_m z A_{m-2}, \quad m = 1, \dots, M \qquad (22)$$

$$B_m(z) = B_{m-1}(z) + d_m z B_{m-2}(z), \quad m = 1, \dots, M \qquad (23)$$

Relations (22) and (23) can be used to evaluate $A_M(z)$ and $B_M(z)$ recursively and with high numerical efficiency. The initial values are:

$$A_{-1}(z) = 0, B_{-1}(z) = 1, A_0(z) = d_0, \text{and } B_0(z) = 1.$$

Finally, from (9):

$$f_n = \frac{2e^{ct}}{T} Re\left\{ \frac{A_M(z)}{B_M(z)} \right\} \qquad (24)$$

Recall that $z = e^{2\pi jn/N}$.

Expression (24) constitutes a basic form for the QD-algorithm being applied to numerically evaluate the inverse Laplace-integral. A further refinement to this algorithm, here in after QD-NLT, is to perform a portion of the summation (14) using an *N*-sample *IFFT* with *N<M*. The remaining terms are incorporated into the partial sum using the QD-algorithm [14]. Considering that *M=N+2J*, and that *N* is of the form $N = 2^\ell$, with ℓ being a positive integer, the QD-acceleration is applied to the last *2J* terms. Thus, initial values for (22) and (23) should now be:

$$A_{N-1}(z) = 0, B_{N-1}(z) = 1, A_N(z) = d_N, \text{and } B_N(z) = 1.$$

VI. APPLICATION CASES.

6.1 Laplace inversion of an analytic expression.

A common practice among NLT methods developers is to test inversion algorithms using a set of Laplace-domain functions whose time-domain counterparts are available in analytic form. Cohen provides a set of 35 of such test functions in [9]. Both the QD-NLT and the W-NLT methods have been tested with all these functions, as well as with the following:

$$F(s) = \frac{se^{-2s}}{s^2 + 1}. \qquad (25)$$

The results from all these test functions are basically identical and only those from expression (25) are presented below. In these authors' experience, the worst case in PS-EMT analysis is with a Laplace function tending asymptotically to $1/|s|$. This is the case for the Laplace transform of a step-function $u(t)$ as well as for *F(s)* in (25). The inverse Laplace transform of (25) is

$$f(t) = \cos(t - 2) \times u(t - 2) \qquad (26)$$

The numerical inversion of (25) is now performed using both the W-NLT and the QD-NLT methods, setting the observation time at $T=20$ s. Damping coefficient c is obtained from (11) by considering an aliasing error-bound of $\epsilon = 10^{-10}$. A number $N=1024$ of frequency-domain samples is used with the W-NLT, while a number $M=1031$ of those samples is used with the QD-NLT (*i.e.*, $J=3$).

Figure 2 shows the plot for analytic function (26) together with the other two numerical results plots obtained with the W-NLT and the QD-NLT methods. The differences among these three plots cannot be seen by the naked eye. Figure 3 shows the relative errors plots for both numerical methods. Relative errors are calculated as follows:

$$\epsilon_{rel,n} = \frac{|f_{ref,n} - f_{num,n}|}{max(f_{ref})}; \; n = 0, 1, 2, \dots, N-1) \qquad (27)$$

where $f_{ref,n}$ is the *n-th* sample of analytic $f(t)$ in (26), $f_{num,n}$ is the *n-th* sample obtained from the numerical method being evaluated, and $max(f_{ref})$ is the maximum value of analytic function $f_{ref}(t)$. Note that $\epsilon_{rel,n}$ is plotted in Fig. 3 on a base-10 logarithmic scale. This figure shows that the overall relative error for the W-NLT is approximately $\epsilon_{rel} = 10^{-4}$, while that for the QD-NLT is $\epsilon_{rel} = 10^{-8}$. Clearly, there are four orders of magnitude-difference between the accuracies of the W-NLT and the QD-NLT methods.
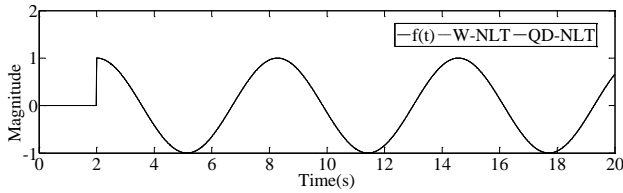

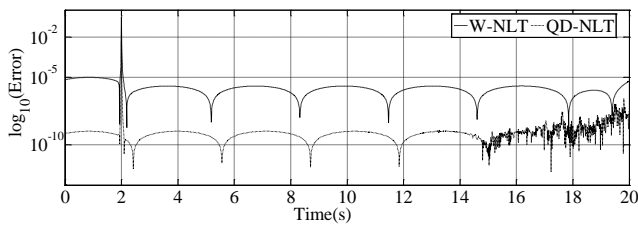*Figure 2. Time-domain image for F(s) given by (24) as obtained analytically and numerically with W-NLT and QD-NLT.*

Figure 3. Differences plot between analytic f(t) and its numerical approximations with W-NLT and QD-NLT.

6.2 EMT response of an aerial power-line.

Figure 4 provides the transversal geometry for an aerial power line of length $L=320$ km that is energized at time $t=0$ in its phase A (left most conductor) with an ideal voltage source

$$v_{0,1}(t) = \cos(120\pi t). \qquad (28)$$

The radius of the phase-conductor is r=1.5 cm with resistivity $\rho_c = 5.3 \times 10^{-8}$ Ωm, the radius of the ground wire is r=0.5 cm with resistivity $\rho_{gw} = 1.78 \times 10^{-7}$ Ω m, and ground resistivity is $\rho_{gnd} = 100$ Ω m. Figure 5 shows the longitudinal layout for the line being considered. Note that the three phase conductors are open-ended at both extremes.
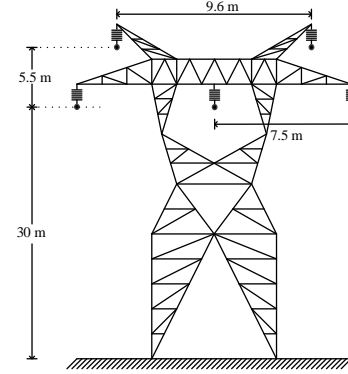

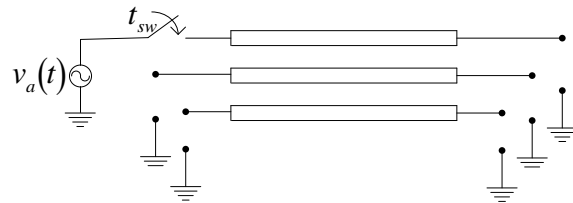*Figure 4. Transversal geometry for the aerial transmission-line case.*

Figure 5. Longitudinal layout for the aerial transmission-line case.

According to the nodal representation of the line, far-end voltages after energizing are given as follows in the Laplace-domain:

$$V_1 = B^{-1}AV_0 \qquad (29)$$

with $A = Y_c coth(\Gamma L)$, $B = Y_c cosech(\Gamma L)$, $\Gamma = \sqrt{YZ}$ and $Y_c = Z^{-1}\Gamma$. Line-parameter matrices Y and Z are calculated as functions of frequency using standard procedures as in [16].

The transient response V_1 given by (29) is now transformed numerically into the time-domain. An observation time T=50 ms is set for this purpose. The number of frequency samples is $N=8096$ and the damping coefficient c is set for an aliasing error-bound $\epsilon = 10^{-9}$. Figure 6 provides the transient responses from the three phase-conductors at the far end, obtained by means of the W-NLT and the QD-NLT. This figure also includes those responses obtained using the EMTP-rv. Again, the differences among results obtained with the three methods cannot be seen by the naked eye. Figure 7 provides the relative difference plots of the W-NLT and the EMTP-rv results with respect to those of the QD-NLT. Expression (27) is used for this purpose, taking the QD-NLT results as reference values f_{ref}. Note also that the differences are plotted in Fig. 7 on a base-10 logarithmic scale.
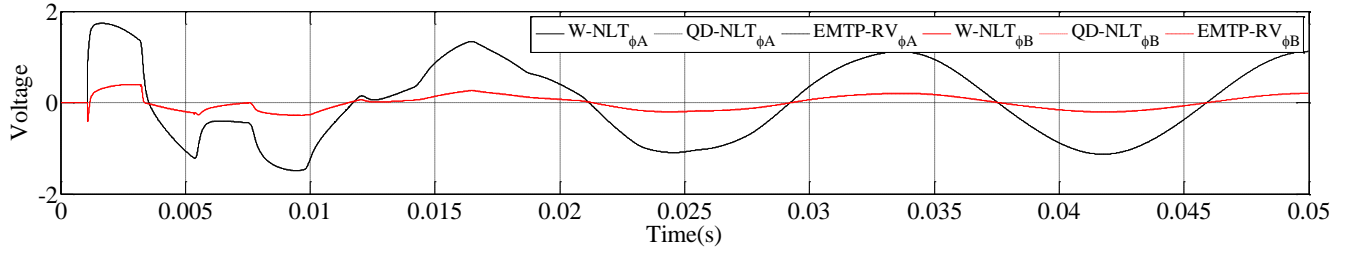
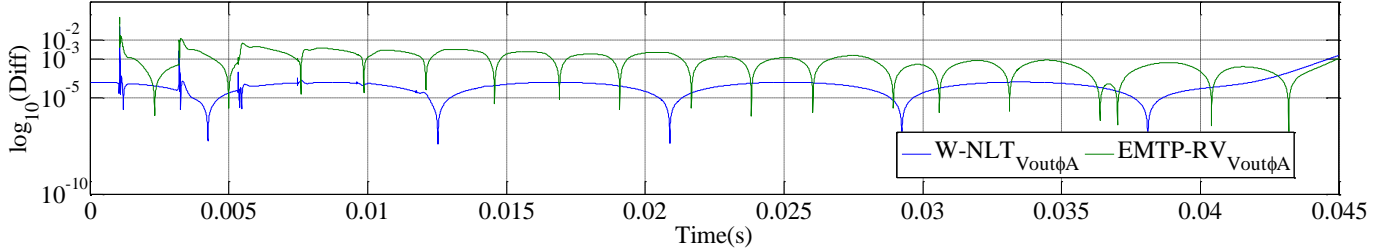*Figure 6. Transient responses at the far-end for the transmission-line case.*

Figure 7. Relative differences plots of W-NLT and EMTP-rv with respect to the QD-NLT for the transmission-line case. Only for far-end phase A

6.3 EMT response from an underground power-cable.

Figure 8 shows the transversal geometry of a three-phase underground transmission cable-system of length *L=5 km*. Each of the three cables is a concentric array with an innermost nucleus, an insulation layer, a sheath, and an outermost insulating protecting-layer. The corresponding radii are provided in the figure. Both insulating layers present a relative permeability $\varepsilon_{rel} = 3$. The respective resistivities for the nuclei and the sheaths are $\rho_n = 1.72 \times 10^{-8}\ \Omega\,m$ and $\rho_{sh} = 1.38 \times 10^{-7}\ \Omega\,m$. The ground resistivity is $\rho_{gnd} = 40\ \Omega\,m$. Figure 9 shows the longitudinal layout of the cable. Note that the three nuclei and sheaths are open-ended at both extremes of the cable. Core A is energized at time *t=0* with an ideal voltage source given by (28).
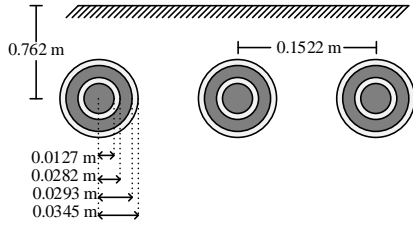

Figure 8. Transversal geometry for the underground transmission-cable case.
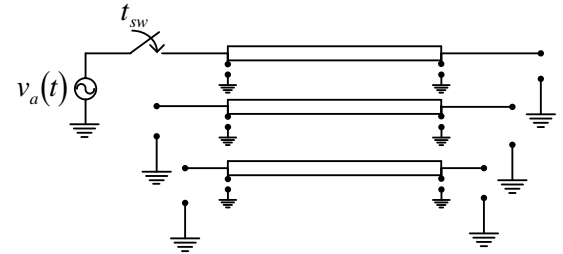

Figure 9. Longitudinal layout for the underground transmission-cable case

The transient responses from the cable system are obtained in the Laplace-domain using relation (29). Far-end responses are then transformed numerically to time domain with the W-NLT and the QD-NLT. For this purpose, the observation time is set at *T=5 ms*, the number of frequency samples is set at *N=8192,* and damping coefficient *c* is set for an aliasing error-bound $\epsilon = 10^{-9}$. Cable parameter-matrices **Y** and **Z** are calculated according to the methods in [17]. The plots so obtained at the far ends of nuclei A and B are provided in Fig. 10. Transient responses are also obtained with the EMTP-rv program, and their plots are included in Fig. 10. As in the previous test-case, differences among the three sets of results cannot be seen by the naked eye.
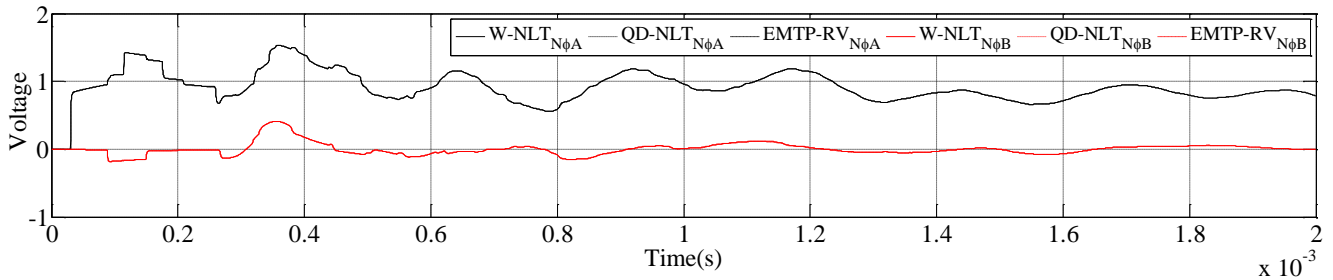

Figure 10. Transient responses at the far-end for nuclei A and B of the transmission-cable case.
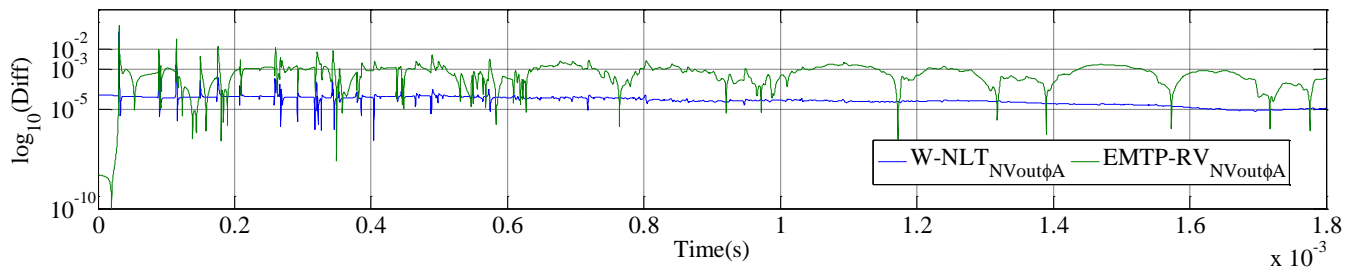
Figure 11. *Relative differences plots of W-NLT and EMTP-rv with respect to the QD-NLT. For far-end phase A only (transmission-cable case).*

Thus, relative-difference plots for W-NLT and for PSCAD/EMTDC, with respect to QD-NLT, are provided in Fig. 11 for nucleus A only, since the results for nuclei B and C are similar.

VII. CONCLUSIONS

The W-NLT method is often used to conduct electromagnetic transient analyses of power systems in the frequency-domain. For most engineering applications, it provides adequate accuracy at moderate computational costs. For research activities, however, much higher accuracy-levels are often required, and these come at an excessive computational cost. In addition to this, high accuracy-levels are not guaranteed with the W-NLT. For this reason, the authors of this paper have introduced an NLT method based on Rutishauser's Quotient-Difference algorithm in this paper [8]. This method has been termed QD-NLT here, and its primary purpose is as a research tool. Application examples provided in this paper have corroborated the high accuracy and moderate computational costs of the QD-NLT method. Comparisons have also been made of the QD-NLT method against the conventional W-NLT method, as well as with a commercial-grade time-domain computer program, the EMTP-rv®. Finally, the authors of this paper consider that the QD-NLT method can still be improved upon substantially and are actively working towards this goal.

VIII. REFERENCES.

[1] J. L. Naredo, J. A Gutiérrez, P. Moreno, A. I. Ramirez, F. A. Uribe, J. L. Guardado, V. H. Ortiz, "Frequency Domain Methods for Electromagnetic Transient Analysis", Proceedings of the 2007 IEEE Power Engineer Society General Meeting, Panel Paper, ISBN: 1-4244-1298-6, Tampa, Fla., USA, June 25-28, 2007.

[2] D. J. Wilcox, "Numerical Laplace Transformation and Inversion", Int. J. of Elect. Enging. Educ., Vol 15, pp. 247-265, 1978.

[3] Wedepohl, L. M. "*Power system transients: Errors incurred in the numerical inversion of the Laplace transform.*" Proc. of the 26th Midwest Symposium on Circuits and Systems, IEEE-MWSCAS, Puebla, Mexico, 1983.

[4] P. Moreno, R. de la Rosa, J. L. Naredo, "Frequency Domain Computations of Transmission Line Closing Transients", IEEE Transactions on Power Delivery, ISSN 0885-8977, Vol. PWRD-6, No. 1, pp 57-63, Jan.1991.

[5] Gómez, Pablo, and Felipe A. Uribe. "*The numerical Laplace transform: An accurate technique for analyzing electromagnetic transients on power system devices*" International Journal of Electrical Power & Energy Systems, Vol. 31, no. 2, pp 116-123, 2009.

[6] M. G. Vega, J. L. Naredo, O. Ramos-Leaños, "*Accuracy Assessment of a Phase Domain Line Model*", Proceedings of the 11th International Conference on Power Systems Transients, IPST'2015, Paper ID 124, Cavtat, Croatia, June 15-18, 2015.

[7] F. R. De Hoog, J. H. Knight, and A. N. Stokes. "*An improved method for numerical inversion of Laplace transforms.*" SIAM Journal on Scientific and Statistical Computing, Vol. 3, No. 3, pp: 357-366 1982.

[8] Rutishauser, Heinz. "*Der quotienten-differenzen-algorithmus.*" Zeitschrift für angewandte Mathematik und Physik ZAMP, Vol. 5, No. 3, pp: 233-251, 1954.

[9] Cohen, A.M. *Numerical methods for Laplace transform inversion*. Springer Science, ISBN 978-0-387-28261-9, New York, U.S.A, 2007.

[10] John G. Proakis, and Dimitris G. Manolakis. Digital signal processing-principles, algorithms and applications . Vol. 2. New York: Macmillan, 1992.

[11] J. L. Naredo, J. Mahseredjian, Ilhan Kocar, J. A. Gutiérrez–Robles and Juan A. Martinez-Velasco, "*Frequency Domain Aspects of Electromagnetic Transient Analysis of Power Systems*", in Transient Analysis of Power Systems ─ Solution Techniques, Tools and Applications, Editor; Juan A. Martínez Velasco, 1st ed., Vol. 1., Chapter 3, Wiley-IEEE Press, pp. 39-71, 2015.

[12] Baker, George A., and Peter Russell Graves-Morris. Padé approximants. Vol. 59. Cambridge University Press, 1996.

[13] Stiefel, Eduard, Peter Henrici, and Heinz Rutishauser. *Further contributions to the solution of simultaneous linear equations and the determination of eigenvalues*. US GovernmentPrint. Office, 1958.

[14] Brancik, L. "*Utilization of quotient-difference algorithm in FFT based numerical ILT method.*" Proceedings 11th Radioelektronica, Brno, Czech Republic pp: 352-355, 2001.

[15] F. Durbin, Numerical Inversion of Laplace transforms: An efficient improvement to Dubner and Abate's method, Computation Journal, Vol. 17, pp: 371-376, 1974.

[16] H. W. Dommel, Electromagnetic transients program reference manual (EMTP Theory Book), Prepared for Bonneville Power Administration (BPA), P. O. Box 3621, Portland OR 97208, USA, 1986.

[17] F. A. Uribe, J. L. Naredo, P. Moreno, L. Guardado, "*Algorithmic Evaluation of underground Cable Earth Impedances*", IEEE Transactions on Power Delivery, ISSN: 0885-8977, Vol. 19, No. 1, pp 316-322, (January, 2004.